

Isotopic portrayal of the Earth's upper mantle flow field

Christine M. Meyzen¹, Janne Blichert-Toft¹, John N. Ludden², Eric Humler³, Catherine Mével⁴ & Francis Albarède¹

It is now well established that oceanic plates sink into the lower mantle at subduction zones, but the reverse process of replacing lost upper-mantle material is not well constrained. Even whether the return flow is strongly localized as narrow upwellings or more broadly distributed remains uncertain. Here we show that the distribution of long-lived radiogenic isotopes along the world's mid-ocean ridges can be used to map geochemical domains, which reflect contrasting refilling modes of the upper mantle. New hafnium isotopic data along the Southwest Indian Ridge delineate a sharp transition between an Indian province with a strong lower-mantle isotopic flavour and a South Atlantic province contaminated by advection of upper-mantle material beneath the lithospheric roots of the Archaean African craton. The upper mantle of both domains appears to be refilled through the seismically defined anomaly underlying South Africa and the Afar plume. Because of the viscous drag exerted by the continental keels, refilling of the upper mantle in the Atlantic and Indian domains appears to be slow and confined to localized upwellings. By contrast, in the unencumbered Pacific domain, upwellings seem comparatively much wider and more rapid.

Radiogenic isotope studies of Sr, Nd and Pb in oceanic islands and mid-ocean ridge basalts (MORB) have established the existence of distinct broad mantle isotopic provinces, such as the archetypal DUPAL anomaly^{1–3}. The distinctive isotopic properties of these large-scale domains are particularly conspicuous in the Sr, Nd, Pb and Hf isotope compositional space of MORB, as shown in Fig. 1. Remarkably, the mantle sources for Indian, South Atlantic, and Pacific MORB are distinct from that of North Atlantic MORB in having lower ε_{Hf} values. Compared to Atlantic and Indian MORB, Pacific MORB on average have lower $^{87}\text{Sr}/^{86}\text{Sr}$ values at a given ε_{Hf} . Indian MORB are characterized by higher $^{207}\text{Pb}/^{206}\text{Pb}$ and $^{208}\text{Pb}/^{206}\text{Pb}$ than their Atlantic and Pacific counterparts. The distinct isotopic identities of each province reflect the long-term segregation of mantle domains composed of various proportions of primordial mantle, melting residues, and recycled components of different ages and origins. Obtaining a clear picture of the transitional regions separating these provinces should help us to understand their genesis and role in global mantle convection patterns. The eastern boundary of the Indian province, which separates the Indian Ocean from the Pacific Ocean mantle domains, has been by far the most closely studied isotopic discontinuity. This boundary, which is located along the Australian–Antarctic Discordance (AAD), is extremely sharp, with $^{206}\text{Pb}/^{204}\text{Pb}$, $^{208}\text{Pb}/^{204}\text{Pb}$, and $^{176}\text{Hf}/^{177}\text{Hf}$ changing dramatically from Indian to Pacific values over less than 25 km on axis^{4,5} (Fig. 2). For this reason, this feature has been interpreted as reflecting a ‘convection front’ overlying either a mantle downwelling⁴, the upwelling of a cold but neutrally buoyant subducted slab associated with a shallow seismic anomaly⁶, or the presence of continental crust remnants⁵.

Because the isotope systematics of MORB from the AAD have proved to be informative about upper-mantle dynamics, we focus here on the isotope characteristics of MORB from the more gradual transition^{7,8} between the Indian and Atlantic domains along the ultraslow Southwest Indian Ridge (SWIR). The occurrence of South-Atlantic-like MORB is mainly restricted to the west of 26° E on this ridge, while Indian-like MORB are present in and to the east

of the Andrew Bain fracture zone ($\sim 30^\circ \text{E}$)^{7,8}. This transition between Indian-like and Atlantic-like mantle sources is broadly centred on the Andrew Bain fracture zone ($\sim 30^\circ \text{E}$). This fracture zone has been proposed to be associated with a diffuse boundary (26.31–32.89° E) separating the African plate into the Nubian and Somalian plates⁹ and we suggest that the distribution of radiogenic tracers along the SWIR is consistent with this view. A previous interpretation of the southward-decreasing $^{176}\text{Hf}/^{177}\text{Hf}$ gradient observed along the Mid-Atlantic Ridge as a consequence of the northwards spilling of mantle material from the Indian Ocean into the Atlantic mantle¹⁰ seems less efficient at explaining this distribution.

Hf and Nd isotope compositions in oceanic basalts are usually well correlated. Their occasional decoupling with respect to the average mantle array, such as along the AAD⁵ or the Mid-Atlantic Ridge north of Iceland¹¹, is symptomatic of unusual fractionation conditions during melting (for example, residual garnet) and thus provides a unique perspective on the dynamics of mantle isotopic provinces. Here, we report new Hf (and some Nd) isotopic compositions for about sixty samples collected between 35° (north of Marion Island) and the Rodrigues triple junction along the neovolcanic zone of the SWIR. These data supplement existing major-element and trace-element¹² and Sr, Nd, and Pb isotope compositions¹³ for the same samples. Here we interpret our new data in the context of global isotopic variability along the mid-ocean ridge system, in particular separating the geochemical signal of hotspots from that of the upper-mantle background. The strongly regionalized character of the asthenospheric isotopic signal is then discussed within the reference frame of the seismic-wave structure of the mantle beneath Africa and is shown to be consistent with the upper-mantle flow field as inferred by ref. 14 from shear-wave splitting and other geophysical observations.

The isotopic transition between Indian and South-Atlantic ridges

To provide a global framework for the examination of the present SWIR data, they were plotted together with Pb, Sr, Nd and Hf isotope data from the PetDB database (www.petdb.org) and other sources

¹Laboratoire des Sciences de la Terre, CNRS UMR 5570, Ecole Normale Supérieure de Lyon, Université Claude Bernard Lyon 1, 46 Allée d'Italie, 69364 Lyon cedex 07, France. ²British Geological Survey, Keyworth, NG12 5GG, Nottingham, UK. ³Laboratoire de Planétologie et Géodynamique, CNRS UMR 6112, Université de Nantes, 2 rue de la Houssinière, B.P. 92208, 44322 Nantes cedex 03, France. ⁴Laboratoire de Géosciences Marines, CNRS UMR 7154, Institut de Physique du Globe, 4 place Jussieu, 75252 Paris cedex 05, France.

(see Supplementary Information) covering the mid-ocean ridge system from the North Atlantic to the Juan de Fuca ridges (Fig. 2). Alternative pathways were possible, such as including the central Indian ridge, but because our primary goal was to obtain a first-order image of the global isotopic variability, we chose to focus on those ridge sections with the densest sampling coverage. This representation depicts, for the first time, the one-dimensional isotopic variability along most of the terrestrial mid-ocean ridge accretionary system. In Fig. 2, the angular distance along the axis was calculated using the successive Euler poles of opening of the consecutive seafloor segments with respect to an arbitrary reference point in the North Atlantic (77.53° N, 7.67° E, see Supplementary Information for explanation of the relevant calculation). The reported isotopic data were first reduced by subtracting the mean value for the entire ridge system and dividing the result by the standard deviation. A new parameter based on Pb isotopes that is particularly suitable for detecting the Indian isotopic affinity of any given sample is also introduced in Fig. 2 with the dual justification that (1) the DUPAL character of the Indian Ocean province is most visible in terms of Pb isotopes¹ (Fig. 1d), and (2) Pb isotope compositions in MORB all fan out from C in Pb isotope space¹⁵ (Fig. 1d). This new parameter R_C was defined as:

$$R_C = \frac{(^{208}\text{Pb}/^{206}\text{Pb}) - (^{208}\text{Pb}/^{206}\text{Pb})_C}{(^{207}\text{Pb}/^{206}\text{Pb}) - (^{207}\text{Pb}/^{206}\text{Pb})_C}$$

in which C refers to the Pb common composition of ref. 15, which is essentially equivalent to the FOZO (Focus Zone) component assigned by ref. 16 to the lower mantle (Fig. 1d). The parameter R_C reflects the time-integrated parent–daughter Th/U ratio in the mantle source of oceanic basalts in much the same way as, for example, $^{143}\text{Nd}/^{144}\text{Nd}$ reflects the Sm/Nd ratio and $^{206}\text{Pb}/^{204}\text{Pb}$ reflects the U/Pb ratio. It thus captures the higher values of $^{208}\text{Pb}/^{206}\text{Pb}$ for a given $^{207}\text{Pb}/^{206}\text{Pb}$,

and hence the higher time-integrated Th/U of Indian Ocean MORB with respect to those of other MORB (Figs 1d and 2).

The diagrams in Fig. 2 have been divided into four main regions: the North and central Atlantic (I), the South Atlantic (II), the southwest and southeast Indian (III), and the Pacific (IV) domains. Regions I and IV will not be discussed in detail here and may admittedly be subdivided further, such as in region I south of the Azores. To assist the discussion, the $^{206}\text{Pb}/^{204}\text{Pb}$ of the C component¹⁵ and the R_C value of the depleted mantle component¹³ are also shown in Fig. 2.

The unradiogenic end of the north–south decreasing gradient of $^{176}\text{Hf}/^{177}\text{Hf}$ defined by Atlantic MORB^{7,10,17} separates the South-Atlantic-like (II) from the southwest-Indian-Ocean-like (III) mantle domains along the SWIR at an angular distance of $\sim 150^\circ$ with respect to the reference point defined above (Fig. 2). This boundary coincides with abrupt changes in R_C , $^{206}\text{Pb}/^{204}\text{Pb}$, and $^{87}\text{Sr}/^{86}\text{Sr}$ and manifests itself in the $^{143}\text{Nd}/^{144}\text{Nd}$ profile as a steep gradient opposite to the gradient in the South Atlantic. The main reason for isolating region II in the South Atlantic from region I in the North Atlantic is the presence of breaks observed north of Tristan da Cunha at $\sim 20^\circ$ S (ref. 18) in the $^{143}\text{Nd}/^{144}\text{Nd}$, $^{87}\text{Sr}/^{86}\text{Sr}$ and R_C profiles.

Unscrambling the hotspot and asthenospheric signals

Interaction of mid-ocean ridges with hotspots has been identified in a number of different localities, such as near Bouvet Island on the southernmost Mid-Atlantic Ridge, the America–Antarctic ridge, and the westernmost SWIR¹⁹, which all exhibit extreme geochemical variability. As will be discussed below, this variability is independent of the nature of the geochemical components present in MORB and in plume magmas. To highlight the effect of hotspots on the isotopic composition of MORB, the standard deviation of each isotopic parameter j (for example, $j = ^{143}\text{Nd}/^{144}\text{Nd}$) was calculated over 5°

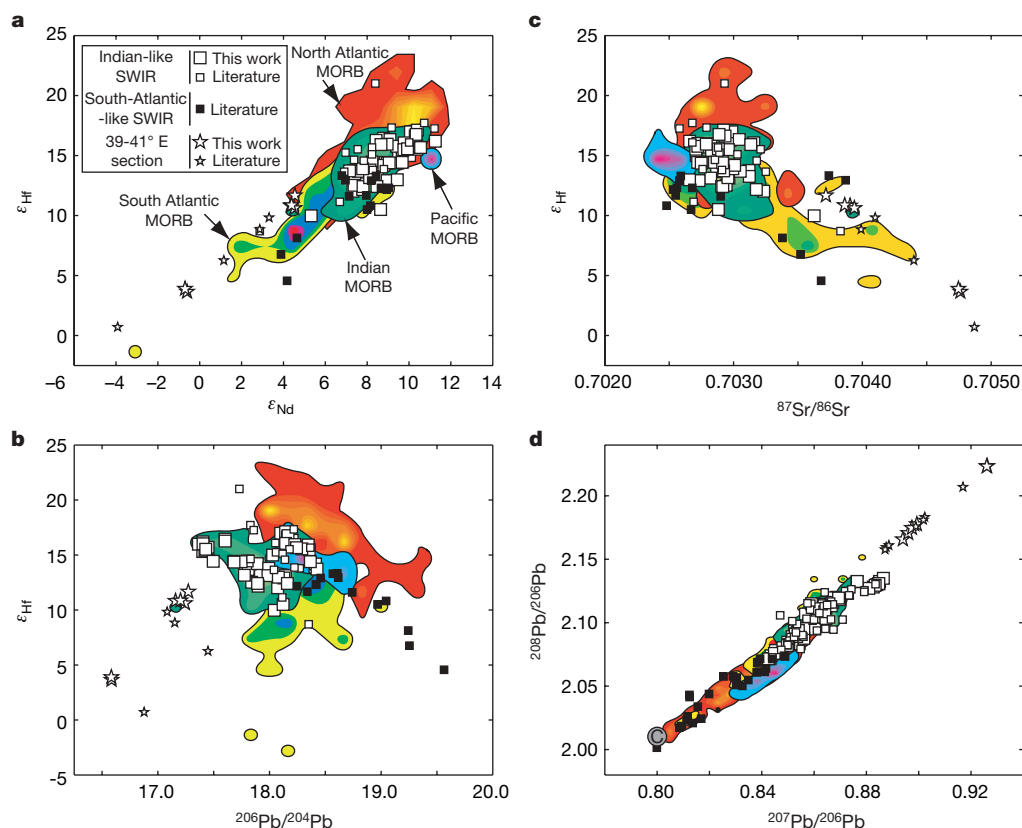


Figure 1 | Isotopic characteristics of SWIR lavas compared to those of other MORB from the Indian, Pacific, South Atlantic and North Atlantic oceans. a, ϵ_{Hf} versus ϵ_{Nd} . b, ϵ_{Hf} versus $^{206}\text{Pb}/^{204}\text{Pb}$. c, ϵ_{Hf} versus $^{87}\text{Sr}/^{86}\text{Sr}$. d, $^{208}\text{Pb}/^{206}\text{Pb}$ versus $^{207}\text{Pb}/^{206}\text{Pb}$. SWIR data for Pb, Sr and Nd isotopes are

from ref. 13. Colour-coded fields are two-dimensional histograms calculated from MORB data retrieved from the PetDB resource and from recent literature (see the Supplementary Information for data sources) as well as the data of this work. C denotes the common component of ref. 15.

intervals i (s_i^j , where $i = 1, 2, \dots$) as a function of the angular distance along the ridge axis and normalized to the total standard \bar{s}_j deviation of the whole MORB population considered in the compilation. Such a representation gives a dimensionless estimate of the local isotopic variability for each parameter (Fig. 3a). The observed isotopic variability is concentrated around a small number of peaks broadly coinciding with the hotspots of the islands of Iceland, the Azores, and the Bouvet, St Paul and Salas y Gomez. With the exception of the ridge section between Tristan da Cunha and Bouvet Island, the background variability is minimal between peaks regularly spaced at $30\text{--}40^\circ$. Spectral analysis is an alternative tool to estimate the hotspot spacing along mid-ocean ridges. The parameter j was first reduced by subtracting the mean value and normalizing to \bar{s}_j . The reduced signals obtained in this way are dimensionless and can therefore be added ('stacked'). The spectra of the reduced signals were then calculated using Lomb–Scargle periodograms, which are suitable for

very irregularly spaced samples²⁰. Because the peak positions look rather similar for each parameter j (see Supplementary Information), only the spectrum of the stacked reduced signals is shown in Fig. 3b.

The three strongest peaks at $1/0.004^\circ$, $1/0.023^\circ$ and $1/0.032^\circ$ correspond to dominant wavelengths at 250° , 43° and 31° , respectively. The signal at 250° reflects the overall larger hotspot abundance in the Atlantic and Indian Oceans relative to the Pacific Ocean. The wave-numbers of the other two peaks are shifted by approximately $(0.032 - 0.023)/2 = 1/0.0045^\circ$, which suggests that the 43° and 31° peaks represent a modulation of a single wavelength at $\sim 35^\circ$ by the 250° signal. The origin of this periodicity is unknown but may reflect the dominance of some particular convective modes (which can be defined as the number of maxima or minima of the upwelling velocity on a great circle) along the mid-ocean ridge system. The signal is, however, strong enough on the isotopic profiles to separate the hotspot signal from its asthenospheric background dominated by

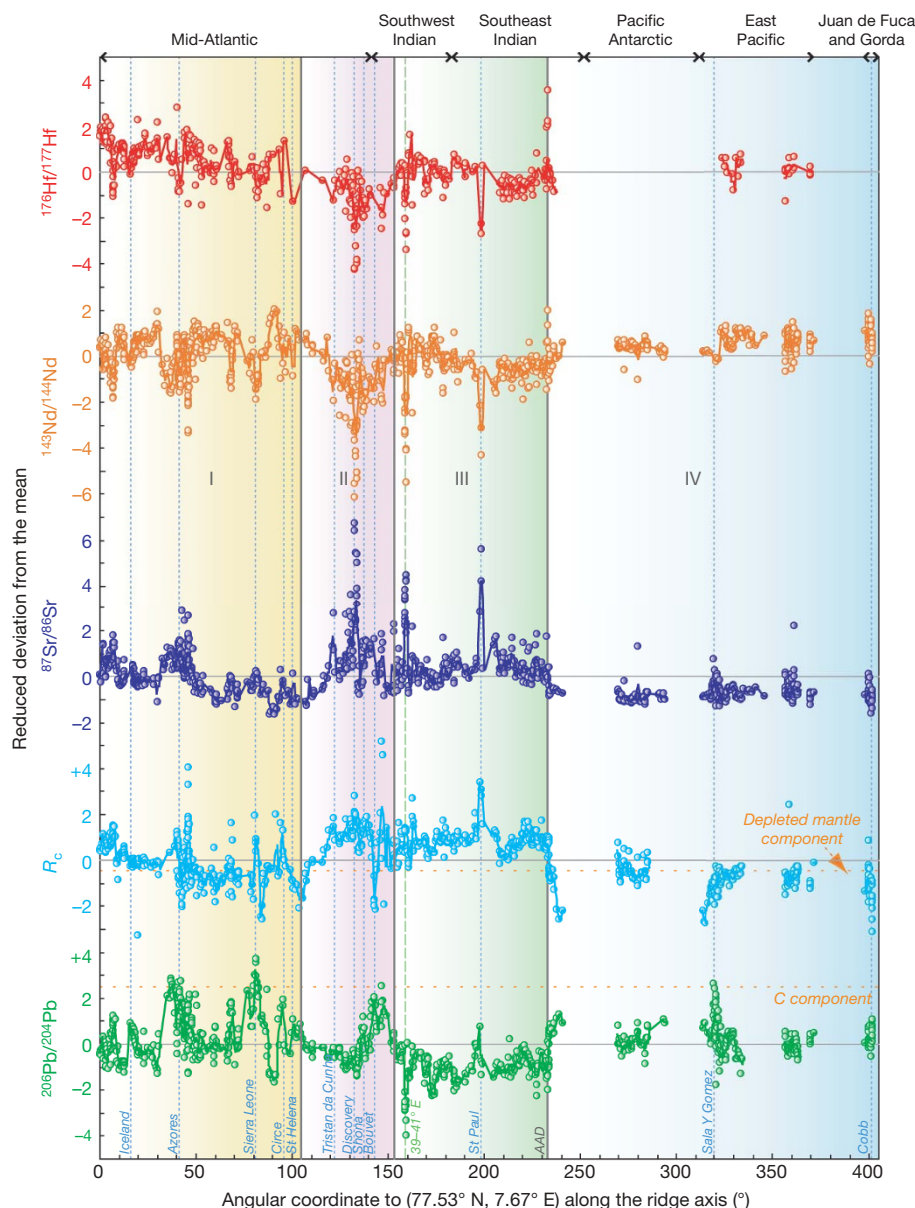


Figure 2 | Variations of $^{176}\text{Hf}/^{177}\text{Hf}$, $^{143}\text{Nd}/^{144}\text{Nd}$, $^{87}\text{Sr}/^{86}\text{Sr}$, R_c and $^{206}\text{Pb}/^{204}\text{Pb}$ along the ridge axis from the North Atlantic to Juan de Fuca. Locations of ridges and major hotspots are also shown, including those of the $39\text{--}41^\circ\text{E}$ section and the AAD. See the Supplementary Information for data description and data sources. The northernmost sample in the Atlantic Ocean (77.53°N , 7.67°E) is the global reference point. Four regions have

been identified: the North and central Atlantic (I), the South Atlantic (II), the Southwest and Southeast Indian (III), and the Pacific (IV). The curve corresponds to a smoothing of the data using a gaussian filter with a 0.5° standard deviation. Points with uncertainties in excess of 20% on R_c have been left out.

geochemically depleted material. Peaks of strong isotopic variability will thus be assigned to hotspots, while the baseline will be considered as representing the MORB source.

Geochemical MORB components

The origin of the geochemical components that define the South Atlantic and Indian 'flavours' of domains II and III, respectively, is not fully understood. The high $^{206}\text{Pb}/^{204}\text{Pb}$ 'HIMU' component, typical of just a small number of islands, such as St Helena, is restricted to the neighbourhood of a few hotspots, such as Shona²¹, and does not seem to be part of the MORB background. The low $^{206}\text{Pb}/^{204}\text{Pb}$ (low $^{238}\text{U}/^{204}\text{Pb}$ or 'LOMU') component has attracted

considerable attention and four interpretations have been put forward, each corresponding to the presence of various components in the MORB source: (1) subducted oceanic crust and sediments^{22–24} and dehydration fluids^{25,26}, (2) debris of subcontinental lithosphere trailing in the asthenosphere after the dislocation of the Gondwana supercontinent over the past 200 million years^{8,21,27–29}, (3) debris of delaminated lower crust^{5,13,30,31} or (4) input from the lower mantle^{2,29}. The presence of subcontinental lithosphere modified by subduction—that is, a combination of interpretations (1) and (2)—was also considered a possibility for the SWIR⁷. A record of ancient subduction processes, dragging down debris from both the oceanic crust and the lower continental crust now stored in the lithospheric keels of Archaean cratons, is provided by the occurrence of eclogites among xenoliths from South African kimberlites³².

Between Bouvet Island and Tristan da Cunha (region II in Fig. 2), the South Atlantic Ridge is underlain by asthenosphere with high $^{87}\text{Sr}/^{86}\text{Sr}$, low $^{143}\text{Nd}/^{144}\text{Nd}$ and $^{176}\text{Hf}/^{177}\text{Hf}$, and high R_C values, suggesting that it has incorporated continental crust debris. However, a strong gradient in Hf isotopes as observed on this segment by refs 10 and 17 indicates that the contribution of continental crust decreases towards the central Atlantic. Likewise, an extreme isotopic variability within the Indian domain, notably between 39 and 41° E of longitude¹³ and on the Indian side of the AAD⁵, hints at a local presence of lower crustal debris trailing in the mantle following the Gondwana break-up.

Apart from these conspicuous but local anomalies, the isotopic properties of the Indian-type MORB upper mantle are inconsistent with the ubiquitous addition of common compositions of a crustal component⁷: Hf is not less radiogenic in Indian MORB than in Pacific MORB and ε_{Hf} does not correlate with $^{87}\text{Sr}/^{86}\text{Sr}$ (Fig. 1). Furthermore, the presence of subducted sediments²⁴ in the source of Indian MORB is incompatible with the unradiogenic Pb^{31,33} of the latter. Rather, the unmistakable common isotopic flavour of ocean island and mid-ocean ridge basalts from the Indian Ocean domain (region III) suggests a deep mantle origin for the overall Indian signature^{2,29} (see Supplementary Information). As is suggested by the extreme geochemical variability of ocean island basalts¹⁸, the lower mantle is certainly not homogeneous. Remarkably, the isotopic compositions of Nd, Sr, Hf and Pb of basalts from the Hawaiian hotspot^{34,35} plot either within the field of Indian MORB of Fig. 1 or at its enriched end and this is also true for some other hotspots. A comparable connection is borne out by the high R_C values of most Indian MORB, which reflect high time-integrated parent–daughter Th/U ratios exactly as in the source of ocean island basalts³⁶ (Fig. 2). A hotspot-like component therefore seems to be present in the Indian Ocean asthenosphere.

Upper-mantle flow field from the Indian and South Atlantic oceans

The mechanisms that led to the establishment in the upper mantle of a huge isotopic province with a lower-mantle signature and occupying most of the Indian upper mantle can be explained by simple geodynamic constraints. It is unlikely that the Indian isotopic province owes its existence to very-low-order modes of mantle convection. The broad latitudinal band of mantle with isotopically similar properties such as hypothesized by ref. 1 is inconsistent with the steep juxtaposition of three isotopic provinces (regions II, III, and IV) at similar latitudes. Furthermore, an order-3 mode (as inferred from ref. 2) in the Southern Hemisphere is incompatible with the strong contrast between both Indian and South Atlantic MORB and Indian and South Pacific MORB and with the sharp transition between these isotopic provinces.

Instead, the provinciality of the Indian Ocean (region III), coupled with its isotopic characteristics, is more consistent with replenishment of the upper mantle through a localized upwelling, a mechanism which is also in agreement with the seismic structure of the underlying mantle. An inclined low-velocity anomaly extends from the core–mantle boundary region beneath the southeastern Atlantic

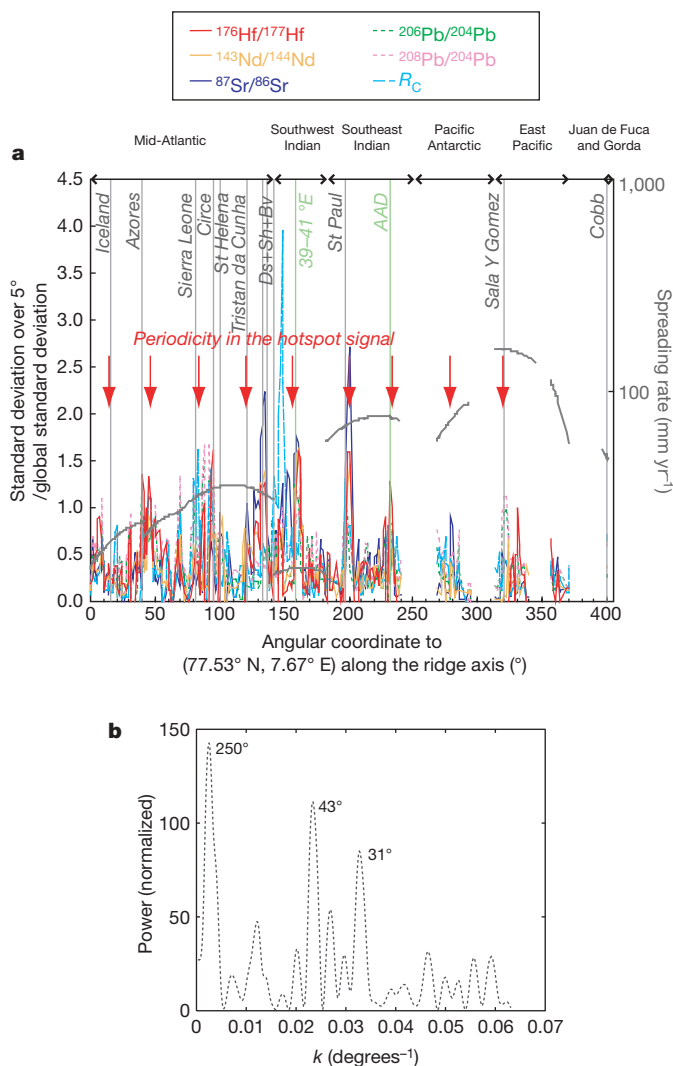


Figure 3 | Spectra of the isotopic signals. **a**, Variations along the ridge axis of the standard deviation of isotopic ratios calculated over 5° intervals and normalized to the global value. Locations of hotspots and mid-ocean ridges are also shown. Ds+Sh+Bv indicates the Discovery, Shona and Bouvet hotspots, respectively. Spreading rates (grey curves) are from ref. 52. This plot shows that (1) with the exception of the segment between Bouvet Island and Tristan da Cunha, the variance peaks are nearly regularly distributed (at 35–40° spacing, red arrows), and (2) there is little or no correlation between isotopic variance and spreading rate. **b**, Plot of the periodograms of the stacked isotopic signals with respect to the wavenumber k in units of inverse degrees. The peak at 250° emphasizes the global contrast between the Pacific and the Atlantic + Indian domains. The two peaks at 43° and 31° represent a modulation of a single wavelength at ~35° by the 250° signal. The 35° signal reflects that the isotopic effect of ridge–hotspot interaction is regularly distributed along the ridge axis. See the Supplementary Information for data sources.

Ocean into the upper mantle beneath East Africa^{37–39}. Using mantle velocity inferences from shear-wave splitting analysis, ref. 14 defined the three-dimensional flow field created by this anomaly and found it to be dominated by a major upwelling originating in the lower mantle beneath southern Africa and radiating along the base of the asthenosphere under the Afar plume. Strong independent support for this model is provided by the presence of an Indian isotopic signature in Gulf of Aden basalts, which are strongly influenced by the Afar plume, at least west of 48° E (ref. 40).

Both geochemical and geophysical evidence therefore confirm that lower-mantle material from the African upwelling flows into the asthenosphere underlying East Africa and the Indian Ocean. The contaminated mixture then spreads southwards along the Indian ridges (Fig. 4) and only reaches the South Atlantic Ridge after first having been deflected under the deep roots of the South African Archaean cratons, extending down to depths in excess of 300 km (refs 41, 42). Continental roots contaminated by old subduction zones or sprinkled with subducted fragments and continental crust³² impart a distinct continental signature on the mantle source of South Atlantic MORB. A similar mechanism has recently been proposed to account for the anomalous isotopic compositions of the Walvis ridge⁴³. The relatively low ³He/⁴He values⁴⁴ observed along the South Atlantic Ridge are consistent with a He contribution from the subcontinental lithospheric mantle, which is known to be more radiogenic than asthenosphere He^{44,45}. Likewise, on the SWIR at 39–41° E, the continental signature of this segment reflects the effect of a southward mantle flow grazing the roots of the Madagascar craton.

The ‘holes-in-the-floor’ model¹⁴, describing exchange of material across the transition zone, is consistent with available geochemical, geodynamic, and geophysical evidence. Upper-mantle material lost to the lower mantle, mostly as rigid plates dragged down by their own weight, is replaced by upwelling of lower-mantle material through ‘holes’ of different dimensions in the 660 km discontinuity, such as that underlying East Africa¹⁴. Ref. 46 argued that mantle does not flow freely across the transition zone, which behaves as a leaky boundary with respect to mantle convection with upwellings penetrating more easily than downwellings⁴⁷. This view is supported by the assessment of mid-mantle heat flow based on seismic tomography, which suggests that plumes account for all upward advective heat transport in the lower mantle that eventually breaks through into the upper mantle⁴⁸.

In addition, the Gondwana supercontinent and its break-up history seem to have played a major role in the building of the

present-day asthenospheric flow field pattern. In ref. 49 the Pacific (Panthalassan, region IV in Fig. 2) domain, which contains only oceanic plates, is opposed to the Atlantic–Indian (Pangean, regions I to III) domain, which contains all the continental plates. Compared to the Pacific domain, the mid-ocean ridges from the South Atlantic and Indian Oceans are characterized by (1) abundant near-ridge hotspots, such as Tristan da Cunha and the Bouvet and St Paul islands, correlated with strong peaks of isotopic variability (Fig. 3a), and (2) slow spreading velocities (Fig. 3a) and therefore weaker heat loss. As argued in ref. 14, the upper mantle in the Gondwana domain is contaminated by multiple upwellings, and the drag exerted by the deep roots of the Archaean cratons strongly perturbs the velocity field. This mechanism is also expressed around the ultraslow SWIR, where the thick keels of the African⁴² and Antarctic cratons resist the asthenospheric flow.

In contrast, the weak isotopic variability and the fast spreading rates observed in the Pacific ridge system (region IV) are best interpreted by the presence of broad upper-mantle upwellings with no hindrance from continental lithosphere. Such a pattern is inconsistent with the focusing of broad upwellings under large expanses of continental lithosphere inferred from their insulating effect on mantle convection^{50,51}. In contrast, the viscous drag exerted by the continental keels seems to oppose the rapid rifting of continents. Erosion of continental keels is, at least under southwestern Africa⁴¹, a slow process. A strong viscous drag also explains why heat builds up in the deep mantle under the South Atlantic Ocean and its neighbouring regions, thereby giving this part of the mantle anomalous seismic properties³⁹ and promoting the generation of a large number of small hotspots.

Received 4 March; accepted 10 May 2007.

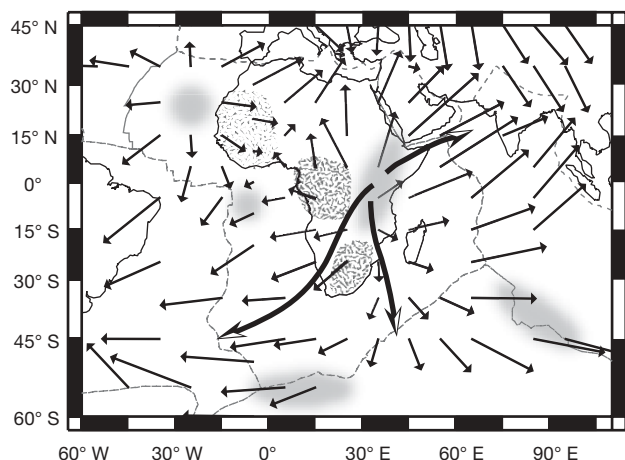


Figure 4 | Map view of the plate- and density-driven flow field at the base of the asthenosphere adapted from figure 7 of ref. 14 with permission. The base of the asthenosphere is at a depth of 300 km. Arrows illustrate horizontal flow. The shaded fields indicate upwellings. Note the radial flow field at the base of the asthenosphere as underlined by bold thick arrows. The patterned areas show the positions of the African cratons.

- Hart, S. R. A large-scale isotope anomaly in the Southern Hemisphere mantle. *Nature* **309**, 753–757 (1984).
- Castillo, P. The DUPAL anomaly as a trace of the upwelling lower mantle. *Nature* **336**, 667–670 (1988).
- Dupré, B. & Allègre, C. Pb–Sr isotope variation in Indian Ocean basalts and mixing phenomena. *Nature* **303**, 142–146 (1983).
- Klein, E. M., Langmuir, C. H., Zindler, A., Staudigel, H. & Hamelin, B. Isotope evidence of mantle convection boundary at the Australian–Antarctic Discordance. *Nature* **333**, 623–629 (1988).
- Hanan, B. B., Blichert-Toft, J., Pyle, D. G. & Christie, D. M. Contrasting origins of the upper mantle revealed by hafnium and lead isotopes from the Southeast Indian Ridge. *Nature* **432**, 91–94 (2004).
- Gurnis, M., Muller, R. D. & Moresi, L. Cretaceous vertical motion of Australia and the Australian–Antarctic Discordance. *Science* **279**, 1499–1504 (1998).
- Janney, P. E., Le Roex, A. P. & Carlson, R. W. Hafnium isotope and trace element constraints on the nature of mantle heterogeneity beneath the Central Southwest Indian Ridge (13°E to 47°E). *J. Petrol.* **46**, 2427–2464 (2005).
- Mahoney, J., Le Roex, A. P., Peng, Z., Fisher, R. L. & Natland, J. H. Southwestern limits of Indian Ocean ridge mantle and origin of low ²⁰⁶Pb/²⁰⁴Pb mid-ocean ridge basalt: Isotope systematics of the Central Southwest Indian Ridge (17–50°E). *J. Geophys. Res.* **97**, 19771–19790 (1992).
- Horner-Johnson, B. C., Gordon, R. G., Cowles, S. M. & Argus, D. F. The angular velocity of Nubia relative to Somalia and the location of the Nubia–Somalia–Antarctica triple junction. *Geophys. J. Int.* **162**, 221–238 (2005).
- Andres, M., Blichert-Toft, J. & Schilling, J.-G. Nature of the depleted upper mantle beneath the Atlantic: evidence from Hf isotopes in normal mid-ocean ridge basalts from 79°N to 55°S. *Earth Planet. Sci. Lett.* **225**, 89–103 (2004).
- Blichert-Toft, J. et al. Geochemical segmentation of the Mid-Atlantic Ridge north of Iceland and ridge-hot spot interaction in the North Atlantic. *Geochem. Geophys. Geosyst.* **6**, Q01E19, doi:10.1029/2004GC000788 (2005).
- Meyzen, C. M., Toplis, M. J., Humler, E., Ludden, J. N. & Mével, C. A discontinuity in mantle composition beneath the Southwest Indian Ridge. *Nature* **421**, 731–733 (2003).
- Meyzen, C. M. et al. New insights into the origin and distribution of the DUPAL isotope anomaly in the Indian Ocean mantle from MORB of the Southwest Indian Ridge. *Geochem. Geophys. Geosyst.* **6**, Q11K11, doi:10.1029/2005GC000979 (2005).
- Behn, M. D., Conrad, C. P. & Silver, P. G. Detection of upper mantle flow associated with the African Superplume. *Earth Planet. Sci. Lett.* **224**, 259–274 (2004).
- Hanan, B. B. & Graham, D. W. Lead and helium isotope evidence from oceanic basalts for a common deep source of mantle plume. *Science* **272**, 991–995 (1996).
- Hart, S. R., Hauri, E. H., Oschmann, L. A. & Whitehead, J. A. Mantle plumes and entrainment—Isotopic evidence. *Science* **256**, 517–520 (1992).

17. Agraniér, A. *et al.* The spectra of isotopic heterogeneities along the Mid-Atlantic Ridge. *Earth Planet. Sci. Lett.* **238**, 96–109 (2005).
18. Hofmann, A. W. in *In The Mantle and Core* (ed. Carlson, R. W.) 61–101 (Treatise on Geochemistry, Holland and Turekian, Oxford, 2003).
19. Kurz, M. D., Le Roex, A. P. & Dick, H. J. B. Isotope geochemistry of the enriched mantle near the Bouvet triple junction. *Geochim. Cosmochim. Acta* **62**, 841–852 (1998).
20. Press, W. H., Flannery, B. P., Teukolsky, S. A. & Vetterling, W. T. *Numerical Recipes: The Art of Scientific Computing* 569–576 (University Press, Cambridge, 1992).
21. Douglass, J., Schilling, J.-G. & Fontignie, D. Plume–ridge interactions of the Discovery and Shona mantle plumes with the southern Mid-Atlantic Ridge (40°S to 55°S). *J. Geophys. Res.* **104**, 2941–2962 (1999).
22. Hamelin, B., Dupré, B. & Allègre, C. J. Pb–Sr–Nd isotopic data of Indian–Ocean ridges—New evidence of large-scale mapping of mantle heterogeneities. *Earth Planet. Sci. Lett.* **76**, 288–298 (1986).
23. Le Roex, A. P., Dick, H. J. B. & Fisher, R. L. Petrology and geochemistry of MORB from 25° to 46°E along the Southwest Indian Ridge—Evidence for contrasting styles of mantle enrichment. *J. Petrol.* **30**, 947–986 (1989).
24. Rehkämpfer, M. & Hofmann, A. W. Recycled ocean crust and sediment in Indian Ocean MORB. *Earth Planet. Sci. Lett.* **147**, 93–106 (1997).
25. Le Roux, P. J. *et al.* Mantle heterogeneity beneath the Southern Mid-Atlantic Ridge: trace element evidence for contamination of ambient asthenospheric mantle. *Earth Planet. Sci. Lett.* **203**, 479–498 (2002).
26. Kempton, P. D. *et al.* Sr–Nd–Pb–Hf isotope results from ODP Leg 187: evidence for mantle dynamics of the Australian–Antarctic Discordance and origin of the Indian MORB source. *Geochem. Geophys. Geosyst.* **3**, doi:10.1029/2002GC000320 (2002).
27. Mahoney, J. J., Natland, J. H., White, W. M., Poreda, R. & Bloomer, S. H. Isotopic and geochemical provinces of the Indian Ocean spreading centers. *J. Geophys. Res.* **94**, 4033–4052 (1989).
28. Andres, M., Blichert-Toft, J. & Schilling, J.-G. Hafnium isotopes in basalts from the southern Mid-Atlantic Ridge from 40°S to 55°S: Discovery and Shona plume–ridge interactions and the role of recycled sediments. *Geochem. Geophys. Geosyst.* **3**, 8502, doi:10.1029/2002GC000324 (2002).
29. Storey, M. *et al.* Contamination of Indian Ocean asthenosphere by the Kerguelen Heard mantle plume. *Nature* **338**, 574–576 (1989).
30. Kamenetsky, V. S. *et al.* Remnants of Gondwanan continental lithosphere in oceanic upper mantle: evidence from the South Atlantic Ridge. *Geology* **29**, 243–246 (2001).
31. Escrig, S., Capmas, F., Dupré, B. & Allègre, C. J. Osmium isotopic constraints on the nature of the DUPAL anomaly from Indian mid-ocean-ridge basalts. *Nature* **431**, 59–63 (2004).
32. Carlson, R. W. *et al.* Continental growth, preservation and modification in southern Africa. *GSA Today* **10**, 1–7 (2000).
33. Zhang, S.-Q. *et al.* Evidence for a widespread Tethyan upper mantle with Indian-ocean-type isotopic characteristics. *J. Petrol.* **46**, 829–858 (2005).
34. Blichert-Toft, J., Frey, F. A. & Albarède, F. Hf isotope evidence for pelagic sediments in the source of Hawaiian basalts. *Science* **285**, 879–882 (1999).
35. Bryce, J. G., DePaolo, D. J. & Lassiter, J. C. Geochemical structure of the Hawaiian plume: Sr, Nd, and Os isotopes in the 2.8 km HSDP-2 section of Mauna Kea volcano. *Geochem. Geophys. Geosyst.* **6**, Q09G18, doi:10.1029/2004GC000809 (2005).
36. Gasperini, D. *et al.* Evidence from Sardinian basalt geochemistry for recycling of plume heads into the earth's mantle. *Nature* **408**, 701–704 (2000).
37. Grand, S. P., VanDerHilst, R. D. & Widiyantoro, S. Global seismic tomography: A snapshot of convection in the Earth. *GSA Today* **7**, 1–6 (1997).
38. Ritsema, J., Ni, S., Helmberger, D. V. & Crotwell, H. P. Evidence for strong shear velocity reductions and velocity gradients in the lower mantle beneath Africa. *Geophys. Res. Lett.* **25**, 4245–4248 (1998).
39. Helmberger, D. V., Ni, S., Wen, L. & Ritsema, J. Seismic evidence for Ultra Low Velocity Zones beneath Africa and Eastern Atlantic. *J. Geophys. Res.* **105**, 23865–23878 (2000).
40. Schilling, J. G., Kingsley, R. H., Hanan, B. H. & McCully, B. L. Nd–Sr–Pb isotopic variations along the Gulf of Aden: Evidence for Afar mantle plume–continental lithosphere interaction. *J. Geophys. Res.* **97**, 10927–10966 (1992).
41. Ritsema, J., Nyblade, A. A., Owens, T. J., Langston, C. A. & VanDecar, J. C. Upper mantle seismic velocity structure beneath Tanzania, East Africa: Implications for the stability of cratonic lithosphere. *J. Geophys. Res.* **103**, 21201–21213 (1998).
42. James, D. E., Fouch, M. J., VanDecar, J. C., Van Der Lee, S. & Group, K. S. Tectospheric structure beneath Southern Africa. *Geophys. Res. Lett.* **28**, 2485–2488 (2001).
43. Class, C. & Le Roex, A. P. Continental material in the shallow oceanic mantle - How does it get there? *Geology* **34**, 129–132 (2006).
44. Graham, D. W. in *Noble Gases in Geochemistry and Cosmochemistry* (eds Porcelli, D., Wieler, R. & Ballentine, C.) 247–318 (Mineralogical Society of America, Washington DC, 2002).
45. Gautheron, C. & Moreira, M. Helium signature of the subcontinental lithospheric mantle. *Earth Planet. Sci. Lett.* **199**, 39–47 (2002).
46. Tackley, P. J., Stevenson, D. J., Glatzmaier, G. A. & Schubert, G. Effects of multiple phase transitions in a 3-dimensional spherical model of convection in Earth's mantle. *J. Geophys. Res.* **99**, 15877–15901 (1994).
47. Tackley, P. J. On the penetration of an endothermic phase transition by upwellings and downwellings. *J. Geophys. Res.* **100**, 15477–15488 (1995).
48. Nolet, G., Karato, S.-I. & Montelli, R. Plume fluxes from seismic tomography. *Earth Planet. Sci. Lett.* **248**, 685–699 (2006).
49. Collins, W. J. Slab pull, mantle convection, and Pangaeian assembly and dispersal. *Earth Planet. Sci. Lett.* **205**, 225–237 (2003).
50. Zhong, S. & Gurnis, M. Dynamic feedback between a continent like raft and thermal convection. *J. Geophys. Res.* **98**, 12219–12232 (1993).
51. Gurnis, M. Large-scale mantle convection and the aggregation and dispersal of supercontinents. *Nature* **332**, 695–699 (1988).
52. Gordon, R. G. *Present Plate Motions and Plate Boundaries* (ed. Ahrens, T.) 66–87 (AGU, Washington, 1995).

Supplementary Information is linked to the online version of the paper at www.nature.com/nature.

Acknowledgements We thank P. Telouk for assistance with the Nu Plasma HR, and B. Reynard, I. Daniel, P. Oger and F. Chambat for suggestions. We also thank M. Behn for providing the map used to draw Fig. 4, J. Ritsema for sharing unpublished seismic profiles, and L. Dosso and B. Hanan for allowing us to view their unpublished data from the Pacific–Antarctic Ridge. Financial support of the analytical work and publication costs were provided by CNRS-INSU (the programmes DyETI and SEDIT), while IPEV provided access to the Marion Dufresne II for sampling during the EDUL (summer 1997) and SWIFT (winter 2001) cruises.

Author Information Reprints and permissions information is available at www.nature.com/reprints. The authors declare no competing financial interests. Correspondence and requests for materials should be addressed to C.M.M. (christine.meyzen@ens-lyon.fr).